AGGREGATED ELECTRONEGATIVE LOW-DENSITY LIPOPROTEIN IN HUMAN PLASMA SHOWS HIGH TENDENCY TO PHOSPHOLIPOLYSIS AND PARTICLE FUSION

Cristina Bancells[1,2], Sandra Villegas[2], Francisco J. Blanco[3,4], Sonia Benítez[1], Isaac Gállego[2], Lorea Beloki[1], Montserrat Pérez-Cuellar[1], Jordi Ordóñez-Llanos[1,2], José Luis Sánchez-Quesada[1]*.

SUPPLEMENTAL DATA

1. Aggregation level

Total LDL(-) had higher turbidity than LDL(+) whereas agLDL(-) presented higher turbidity than nagLDL(-) (Figure 1A-S). Figure 1B-S shows a representative GGE of LDL(+) and LDL(-) fractions, where lipoproteins run according to their size, allowing discrimination between aggregated and non-aggregated LDL particles. The aggregated particles are observed in total LDL(-) and are much more abundant in agLDL(-). It is interesting to note that although agLDL(-) should contain only aggregated particles some monomer particles were also observed in GGE. In turn, nagLDL(-) also showed a minor population of aggregated particles.

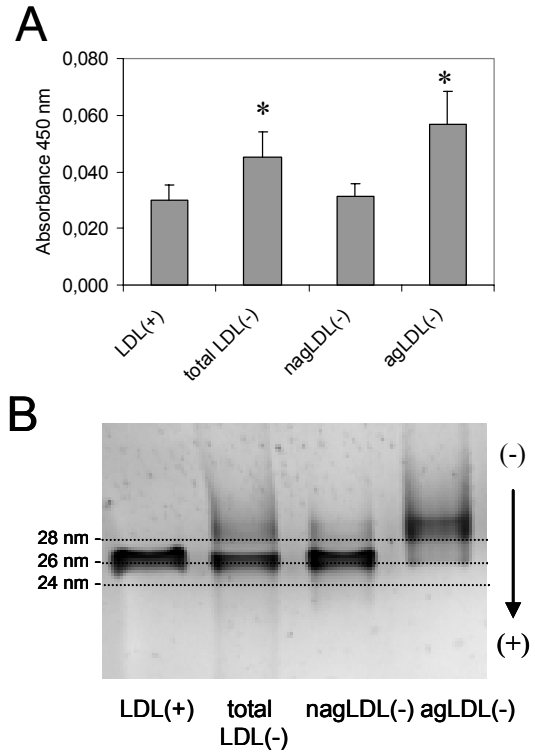

Figure 1S. Turbidity (A) and non-denaturing gradient gel electrophoresis (GGE) (B) of LDL(+) and LDL(-) fractions. (A) LDL subfraction turbidity was measured at 450 nm using 100 μL of LDLs at 0.15 g protein/L. Data are the mean±SD of 6 independent experiments. * indicates $P<0.05$ versus LDL(+) or nagLDL(-). (B) GGE was performed at 100 V for 8 h with 5 μg protein/lane and the gel was stained with Coomassie Brilliant Blue. A representative GGE is shown.

2. Evidence that agLDL(-) was not formed during isolation procedures due to high ionic strength and/or ultracentrifugation shear forces.

2.1. High ionic strength.

The possibility that agLDL(-) could be an artifact formed during isolation procedures due to the high ionic strength used to isolate LDL (at a density of 1.050 g/mL the concentration of KBr is 550 mmol/L and the conductivity is 71.6 mS/cm) was evaluated by skipping the second step of ultracentrifugation and the anion exchange chromatography. VLDL+IDL were isolated at 1.019 g/mL (160 mmol/L KBr and 34.3 mS/cm) and the infranatant containing the rest of plasma proteins (LDL+HDL+LPDS) was fractionated by gel-filtration chromatography. The total time of this procedure, from blood extraction to gel-filtration chromatography was 9 h. The first peak, corresponding mainly to LDL, showed an inflexion in its initial slope (Figure 2A-S) that formed a small but distinct peak at the same elution time than agLDL(-) was isolated by the regular procedure (see Figure 1B). The chromatogram in Figure 2A-S is representative of 6 independent samples. These fractions (tubes B1-B3) were pooled, concentrated and assayed for lipid composition and PLC-like activity. Fractions B4-B10, corresponding to nagLDL, were also pooled and concentrated. The cholesterol/triglyceride molar ratio in B1-B3 and B4-B10 (B1-B3: 5.8±3.3; B4-B10: 12.9±3.4, n=3) was similar to that shown in Table 1 (molar ratio calculated from data in Table 1: LDL(+): 14.9; total LDL(-): 9.4; nagLDL(-): 12.3; agLDL(-): 5.8). These data indicate that the fraction B1-B3 was not VLDL (molar ratio in VLDL is below 1). Figure 2B-S and 2C-S show the PLC-like activity measured by the Amplex Red method (Figure 2B-S) and the BODIPY-SM method (Figure 2C-S), respectively. Both methods showed increased PLC-like activity in the fraction B1-B3 (agLDL) compared to fraction B4-B10 (bulk of nagLDL).

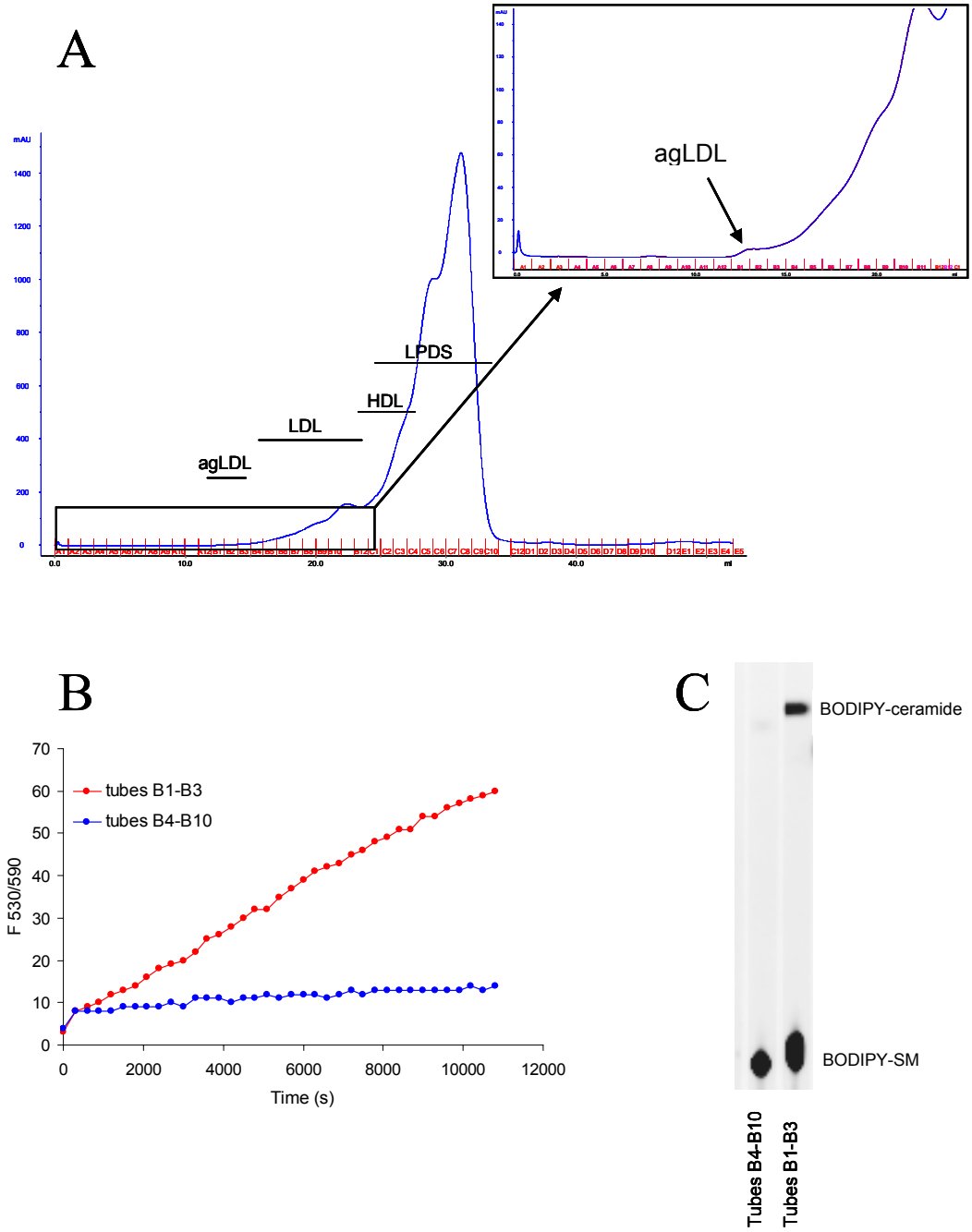

Figure 2S. A) Representative gel-filtration chromatography of plasma depleted of VLDL+IDL. The insert shows the peak corresponding to agLDL. **B) PLC-like activity of agLDL and the bulk of nagLDL by the Amplex Red method.** Fractions B1-B3 (agLDL) and B4-B10 (bulk of nagLDL) were assayed for PLC-like activity using de Amplex Red method, as described in Experimental Procedures, using 50 µL of sample at 0.2 mmol/L cholesterol. The increase of fluorescence indicates the PLC-like activity. **C) PLC-like activity of agLDL and the bulk of nagLDL by the BODIPY-SM method.** Fractions B1-B3 (agLDL) and B4-B10 (bulk of nagLDL) were assayed for PLC-like activity using de BODIPY-SM method, as described in Experimental Procedures. The concentration of the samples was the same than in the Amplex Red method.

2.2. Shear force.

LDL(+) isolated by the regular method was depleted of aggregated forms by gel-filtration chromatography (nagLDL(+)). nagLDL(+) was then re-isolated by ultracentrifugation. To reproduce the same experimental conditions, nagLDL(+) was mixed with the same fractions of VLDL, IDL, HDL+LPDS previously isolated, and at the same proportion as in the original plasma. In addition, nagLDL(+) was re-isolated alone. This second purification again included two ultracentrifugations, the first at 1.019 g/mL to separate VLDL+IDL fractions, and the second at 1.050 g/mL to float LDL. Re-isolated nagLDL(+) was chromatographied by gel filtration.

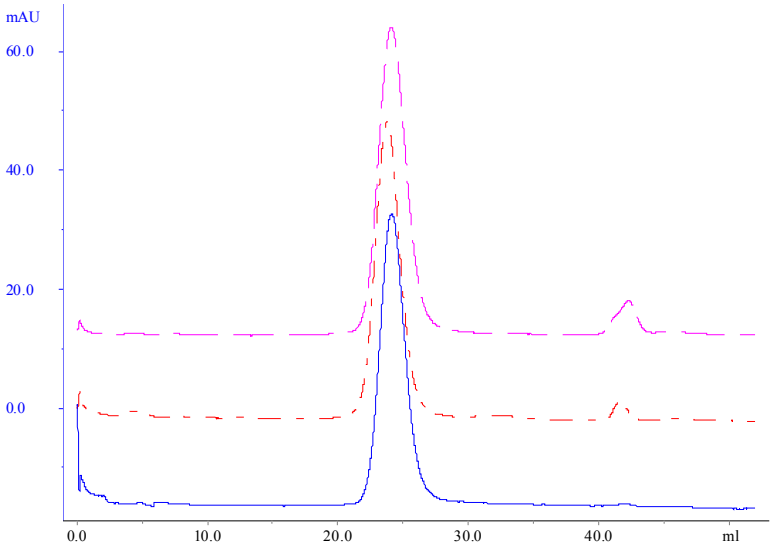

Figure 3S. Gel-filtration chromatograms of nagLDL(+), nagLDL(+) re-isolated from VLDL+IDL+HDL+LPDS and nagLDL(+) re-isolated alone. Blue line: nagLDL(+), red line: nagLDL(+) re-isolated alone; pink line: nagLDL(+) re-isolated in the presence of VLDL+IDL+HDL+LPDS.

No evidence of aggregated LDL formation was observed (Figure 3S), either when LDL(+) was re-isolated alone or in the presence of VLDL+IDL+HDL+LPDS. These results suggest that agLDL(-) was not formed as a consequence of high salt concentration or shear forces during ultracentrifugation and strongly support that this minor LDL subfraction is present in blood.

3. Oxidative characteristics

3.1. Oxidation level

The oxidative level of LDL subfractions was estimated by measuring the ratio of the PC peak areas at 234 nm (corresponding to conjugated dienes) and 205 nm (corresponding to the maximum of absorbance of PC) and by quantification of the α-tocopherol content. In contrast to "in vitro" oxidized LDL, which presented a much lower 205/234 PC ratio and α-tocopherol content, no difference between LDL subfractions was observed (Table 1S).

Table 1S. Oxidation-related parameters of LDL subfractions and "in vitro" oxidized LDL.

	LDL(+)	nagLDL(-)	agLDL(-)	oxLDL
205/234 nm PC ratio*	73.1±1.2	74.5±4.8	74.7±2.4	8.6±1.4
α-tocopherol (mol/mol apoB)*	9.1±1.5	9.0±0.9	10.4±0.4	0.8±0.1
Increase of lag phase vs LDL(+) (%)†	0	43±15	447±281	-

Data are the mean±SD of 3 independent experiments.
* Oxidized LDL (oxLDL) was modified "in vitro" by incubation with 5 μmol/L $CuSO_4$ for 24 h at 37ºC.
† Lag phase time was calculated from the kinetics of conjugated diene formation induced by 5 μM $CuSO_4$, as described in Experimental Procedures.

3.2. Susceptibility to oxidation

The evaluation of LDL susceptibility to $CuSO_4$-induced oxidation showed that LDL(+) was more susceptible to oxidation than nagLDL(-), in agreement with previous observations with total LDL(-),(1) whereas agLDL(-) was much more resistant than LDL(+) and nagLDL(-). Representative conjugated diene kinetics is shown in Figure 4S. The % of increase of the conjugated diene kinetics lag phase-time is shown in Table 1S.

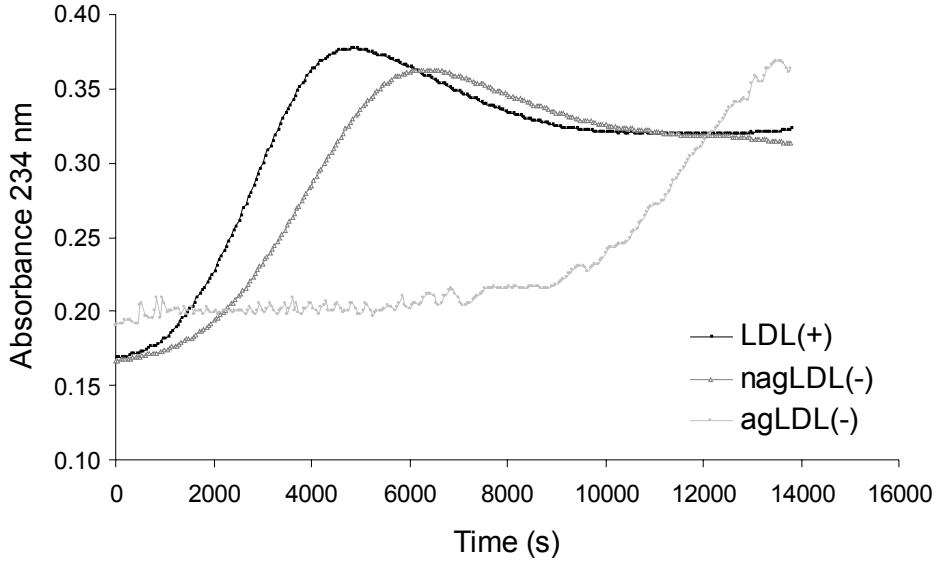

Figure 4S. LDL susceptibility to oxidation: Representative experiment of LDL susceptibility to $CuSO_4$-induced oxidation. LDLs dialyzed in PBS were incubated with $CuSO_4$ and the formation of conjugated diene was monitored at 234 nm, as described in Experimental Procedures.

4. Particle size distribution analyzed by TEM

Before α-chimotrypsin-mediated proteolysis, LDL(+) showed a typical unimodal distribution with predominant particles of intermediate size (25-27 nm) whereas both LDL(-) subfractions showed a bimodal distribution with abundant small and large particles (Figure 5S). This distribution agrees with previous data of density distribution of LDL(-) (2). Assuming that LDL is spherical, two particles with an individual diameter of 25-28 nm would measure 30.4-35.3 nm when both are fused (the yellow bar would indicate the limit between monomer and fused particles). Fused particles were scarce in all LDL subfractions before proteolysis. Proteolysis promoted a massive generation of fused particles but this process was much faster in agLDL(-).

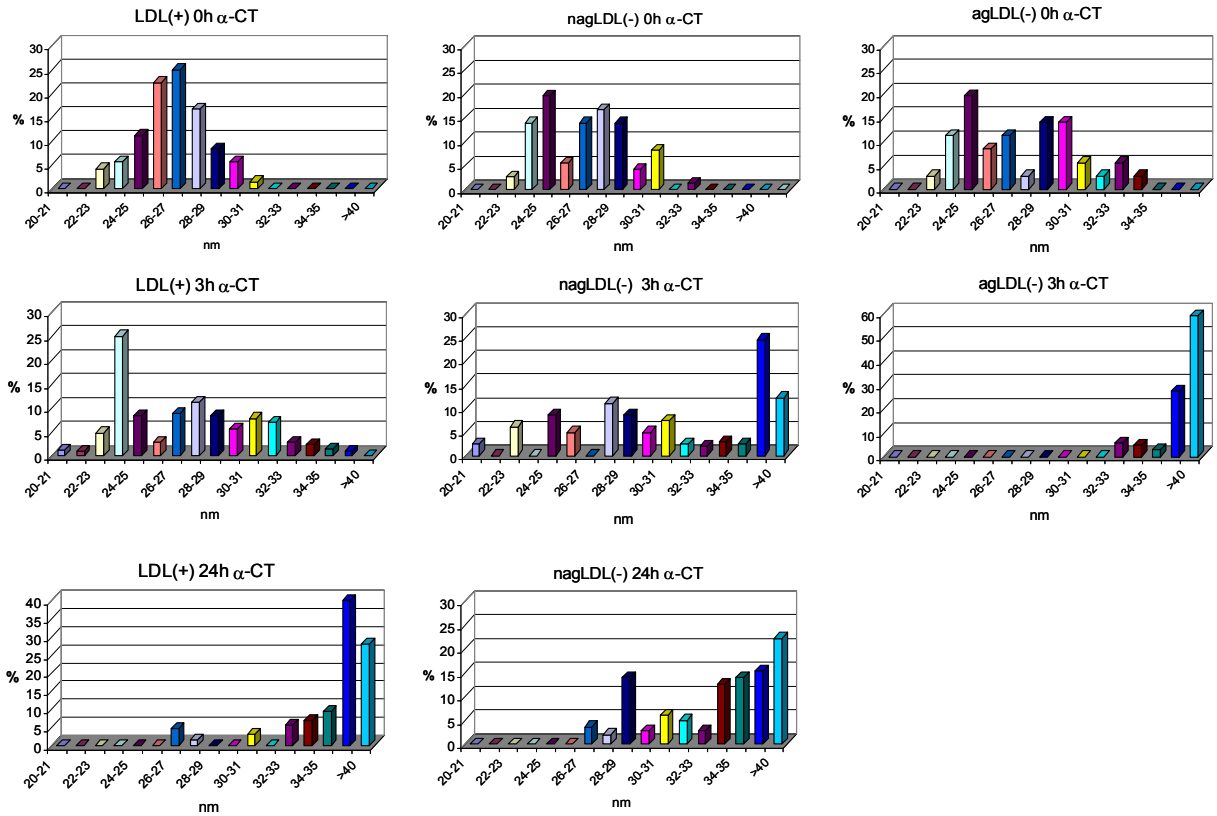

Figure 5S. Size distribution of LDL particles. The diameter of 100 randomly selected particles was measured by TEM at different times of particle fusion induced by α-chymotrypsin proteolysis. agLDL(-) at 24 h of proteolysis could not be measured due to particle degradation.

5. ^{1}H-NMR.

The intensity of the signals corresponding to PC (3.235 ppm) and SM (3.220 ppm)(3,4) decreased progressively in LDL(+) and nagLDL(-), indicating a mild and slow degradation of both phospholipids (Figure 6S). These spectra were similar in LDL(+) and nagLDL(-) with the only difference being a minor signal at 3.185 ppm in nagLDL(-) in the late stages of proteolysis. In contrast, agLDL(-) presented a strikingly different behavior. PC and SM were degraded much faster than in the case of LDL(+) and nagLDL(-); after 6 h of proteolysis the SM signal disappeared, indicating SM degradation, whereas PC presented a strong shift up to 3.260 ppm. This strong shift of PC resonance would reflect changes in the microenvironment of PC molecules during proteolysis. On the other hand, a signal corresponding to LPC (3.230 ppm)(3) was clearly observed after 1 hour of proteolysis but disappeared at 8 h. Instead, two strong signals corresponding to phosphorylcholine (P-choline) (3.200 ppm) and free choline (3.185 ppm)(4) increased progressively during proteolysis. The signal corresponding to P-choline appeared early in the 30-minutes spectrum, increased to its maximum signal at 8 h and then decreased. The signal of free choline appeared after a delay of 4 h and increased continuously up to 24 h.

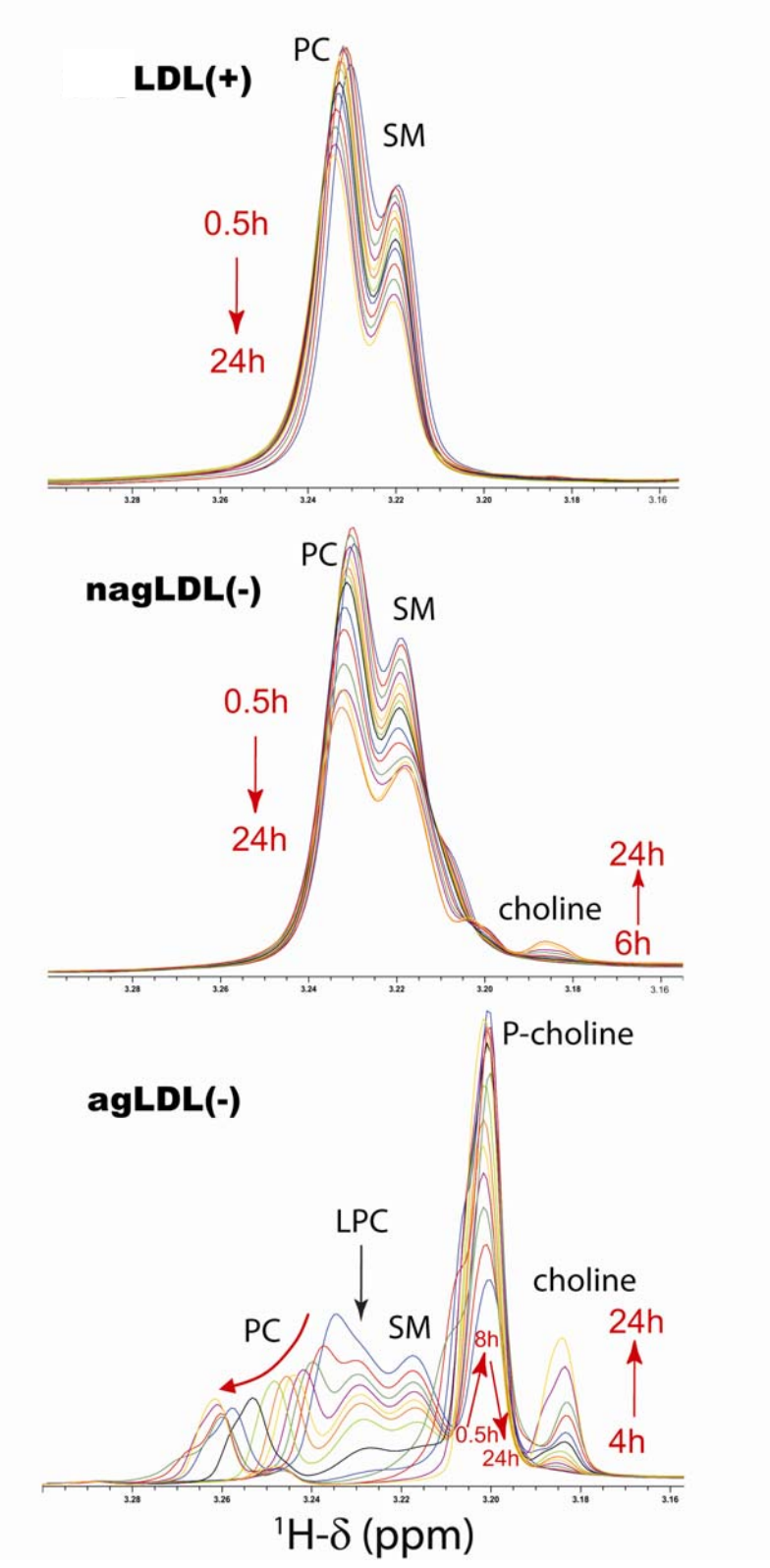

Figure 6S. Overlay of the regions with the choline resonances in ^{1}H NMR spectra of LDL at different times of particle fusion induced by α-chymotrypsin proteolysis. LDLs were mixed with α-chymotrypsin inside the NMR tube and spectra recorded at 37ºC at intervals of 0.5 h, as described in Experimental Procedures. The spectra shown correspond to 0.5, 1, 1.5, 2, 2.5, 3, 4, 6, 8, 12, 16, 20 and 24 h after α-chymotrypsin addition. PC: phosphatidylcholine; SM: sphingomyelin; LPC: lysophosphatidylcholine; P-choline: phosphorylcholine.

Regarding the resonances of ceramide (Figure 7S), the spectra of LDL(+) shows a signal at 5.280 ppm that decreases in intensity and shifts up to 5.300 ppm after proteolysis. The corresponding signal in nagLDL(-) also shifts up to 5.300 ppm but the initial decrease in intensity is reverted after 8 h of proteolysis. The proteolysis of agLDL(-) causes a more complex transition, with a larger shift and a different overall pattern of intensities. The initial signal was observed at 5.290 ppm and shifted to 5.310-5.320 ppm. Indeed, its intensity increased strongly after 8 h of proteolysis.

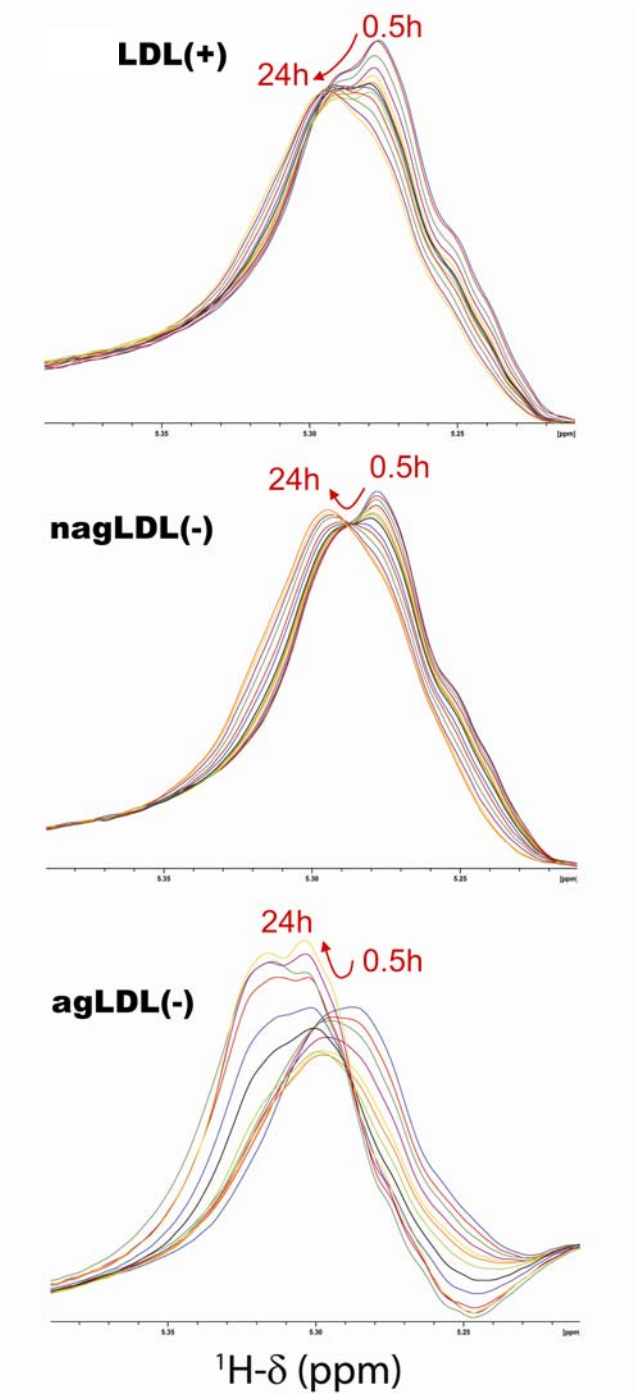

Figure 7S. Overlay of the regions with the ceramide resonances in ^{1}H NMR spectra of LDL at different times of particle fusion induced by α-chymotrypsin proteolysis. LDLs were mixed with α-chymotrypsin inside the NMR tube and spectra recorded at 37ºC at intervals of 0.5 h, as described in Experimental Procedures. The spectra shown correspond to the same time points as in Figure 6S and with the same color code.

The possibility that the behavior of agLDL(-) could be due to extensive oxidation was ruled out by the measurements on the resonance signals at 2.650-2.850 ppm, corresponding to bisallylic compounds (mainly linoleic and arachidonic acids) (Figure 8S).(5) A decrease was observed in all LDL subfractions in the early phases of fusion (less than 3 h), with small shifts. Surprisingly, the overall intensity of the signals increased in agLDL(-), but not in nagLDL(-) or LDL(+), after 4 h of proteolysis.

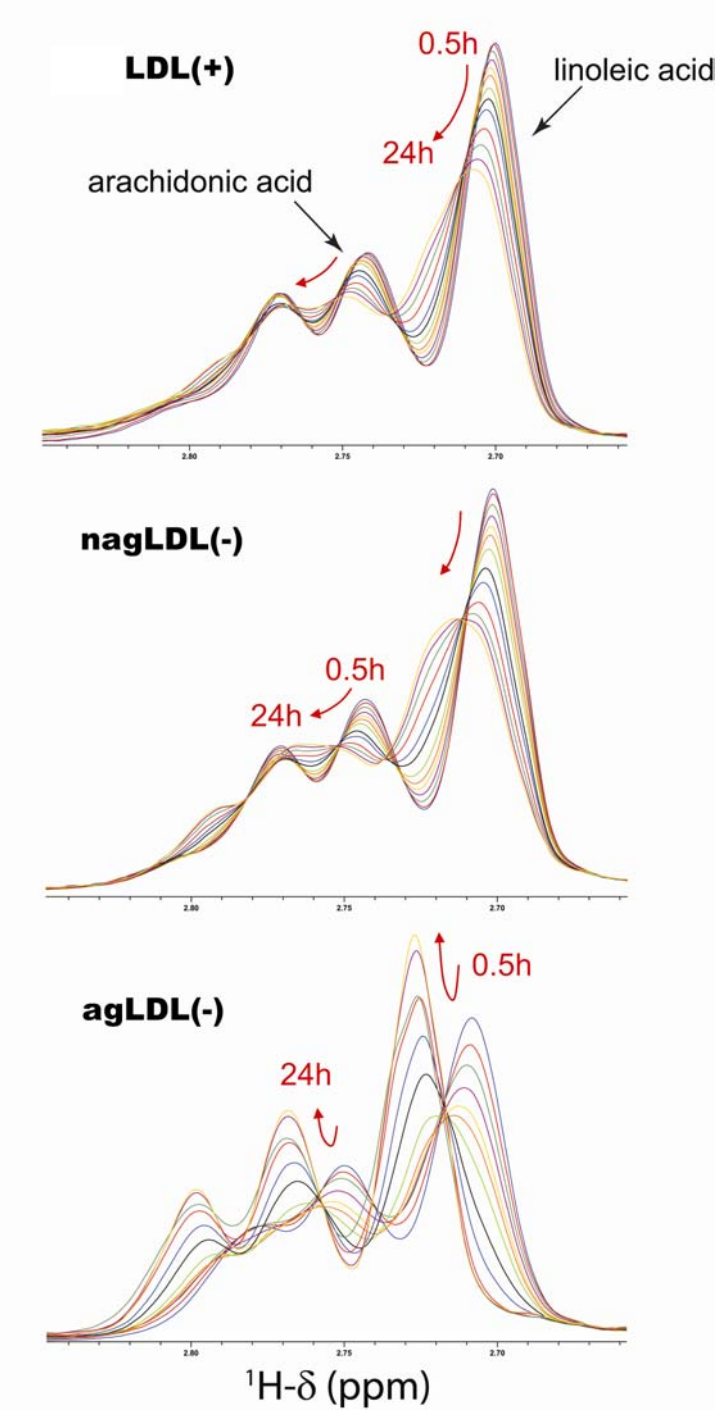

Figure 8S. Overlay of the regions with the bisallylic compound resonances in ^{1}H NMR spectra of LDL at different times of particle fusion induced by α-chymotrypsin proteolysis. A) LDL(+), B) nagLDL(-), C) agLDL(-). LDLs were mixed with α-chymotrypsin inside the NMR tube and spectra recorded at 37ºC at intervals of 0.5 h, as described in Experimental Procedures. The spectra shown correspond to the same time points as in figures 6S and 7S, and with the same color code.

REFERENCES

1. Sanchez-Quesada, J. L., Camacho, M., Anton, R., Benitez, S., Vila, L., and Ordonez-Llanos, J. (2003) *Atherosclerosis* **166**, 261-270
2. Sanchez-Quesada, J. L., Benitez, S., Otal, C., Franco, M., Blanco-Vaca, F., and Ordonez-Llanos, J. (2002) *J Lipid Res* **43**, 699-705
3. Soininen, P., Oorni, K., Maaheimo, H., Laatikainen, R., Kovanen, P. T., Kaski, K., and Ala-Korpela, M. (2007) *Biochem Biophys Res Commun* **360**, 290-294
4. Duarte, I. F., Marques, J., Ladeirinha, A. F., Rocha, C., Lamego, I., Calheiros, R., Silva, T. M., Marques, M. P., Melo, J. B., Carreira, I. M., and Gil, A. M. (2009) *Anal Chem* **81**, 5023-5032
5. Lodge, J. K., Sadler, P. J., Kus, M. L., and Winyard, P. G. (1995) *Biochim Biophys Acta* **1256**, 130-140